OPTIMIZED PSEUDO-DERIVATIVE FEEDBACK WITH FEED-FORWARD CONTROLLER USING FLOWER POLLINATION ALGORITHM FOR AUTOMATIC GENERATION CONTROL IN A RESTRUCTURED POWER SYSTEM

G. Ganesan @ Subramanian[1], I.A. Chidambaram[2] , J.Samuel Manoharan[3]

[1]Research Scholar, Department of Electrical Engineering, Faculty of Engineering and Technology,

Annamalai University, Chidambaram, Tamilnadu, India; email: g.ganeshsubramanian@yahoo.com

[2] Professor, Department of Electrical Engineering, Faculty of Engineering and Te 1234chnology,

Annamalai University, Chidambaram, Tamilnadu, India; email:driacd

@yahoo.com

[3] Professor, Department of Electronics and Communication Engineering, Bharathiyar College of Engineering and Technology, Karaikal, India; email:samuel1530@gmail.com

Abstract: *This paper presents Pseudo-Derivative Feedback with Feed-forward controller (PDFF) controller based Automatic Generation Control (AGC) of a two area interconnected power system. The control parameter of PDFF controller are optimized employing Flower Pollination Algorithm (FPA) in order to achieve the optimal transient response of the test system under for different types of possible transactions in restructured environment. The proposed PDFF controller are used in AGC application which locates the zero at an optimal place that shortens the step response rise time without overshoot and gives better dynamic performance of the system over PI controller. Integral Square Error (ISE) criterion of the test system was considered as an objective function to be minimized for tuning the gains of PDFF controller using FPA. In this study two type of test system is considered such as two area Hydro-Thermal and Thermal-Diesel power system. The simulation results show that the proposed FPA tuned PDFF controller improves the dynamic response of the restructured power system. The convergence speed performance of the proposed FPA algorithm is significantly better compared to those achieved by the existing algorithms. Moreover the Power System Restoration Indices (PSRI) is computed based on system dynamic performances and the remedial measures to be taken can be adjudged. These PSRI indicates that the ancillary service requirement to improve the efficiency of the physical operation of the power system with the increased transmission capacity in the network.*

Key words: *Automatic Generation Control, Flower Pollination Algorithm, Diesel power plant, PDFF Controller, Power System Restoration Indices.*

1. INTRODUCTION

Automatic generation control (AGC) has greater currency in power system operation and control to supply sufficient, efficient, reliable and quality electrical power to the consumers. A critical up-to-date literature review explaining all aspects of AGC is reported in [1–3]. A power system can be considered as being divided into control areas interconnected by the tie-lines. For satisfactory operation of a power system the frequency should

remain nearly constant under fluctuating load demands. AGC system adjusts the generator set point by changing speed changer settings automatically to compensate the mismatch between total generation and total load demand plus associated system losses. The AGC system sustains the scheduled system frequency and established interchange with other control areas within predetermined limits during normal/abnormal operating conditions [4]. In the deregulated structure, several independent entities like distribution companies (DISCOs), generation companies (GENCOs), transmission companies (TRANSCOs) and independent system operator (ISO) have been introduced [5, 6]. ISO is independent, disassociated agent for market participants who perform various ancillary services and among them is the AGC [7]. In open market scenario consumers have a choice to choose among DISCOs in their area, while DISCOs of an area have the freedom to have power contracts for transaction of power with GENCOs of the same or other area.

It is perceived in the power system that parameter values in the various power generating units, viz. governors, turbines, generators etc., are endlessly varying w.r.t time subject to system and power flow condition. Thus, the controller parameters design at normal operation may not able to give satisfactory performance under external disturbed and/or parameter uncertainty condition. To ensure robustness and to preserve the system stability, various populations based meta-heuristic optimization techniques such as Particle Swarm Optimization (PSO) [8], Genetic Algorithm (GA) [9], Biogeography-Based Optimization (BBO) [10], Krill Herd Algorithm (KHA) [11], Teaching Learning Based Optimization (TLBO) [12] and Bacterial Foraging Optimization (BFO) algorithm [13]. were proposed in the literature. From literature survey the enhancement of power system performance not only depends on the control structure but also on the well-tuned controllers. For this purpose, a number of artificial optimization techniques are utilized. So a new high performance heuristic optimization algorithm is always welcome to solve real world problems. Flower Pollination Algorithm (FPA) is a newly developed heuristic optimization method based on Pollination of flowers. It has only one key parameter p (switch probability) which makes the algorithm easier to implement and faster to reach optimum solution [14, 15]. FPA has special capabilities such as extensive domain search with quality and consistency solution [16]

Classical controllers are the first stage closed loop controllers designed for overcome the limitations of open loop control system. The performances for Integral (I), Proportional–Integral (PI), Integral–Derivative (ID), and Proportional-Integral-Derivative (PID) controllers in AGC are practically the same from the viewpoint of dynamic responses [17]. However, the proposed Pseudo-Derivative Feedback with Feed-forward controller (PDFF) provides much better response than the aforesaid controllers. In this study PDFF controllers are designed and implemented using FPA algorithm in AGC loop of the interconnected restructured power system. The experimental results showed that the accuracy and speed performance of the PDFF controller had outperformed the other PI controller.

The modern power system is pushed close to critical operating limits in the market environment. High capacity and long transmission networks are widely used to meet the power supply demand of modern society. Large-scale blackout risks still exist and are inevitable, although a great amount of work has been done to make power systems resilient against outages [18]. A proper restoration plan can effectively mitigate the negative impact on the public, the economy, and the power system itself. The objectives of restoration are to enable the power system to return to normal conditions securely and rapidly, minimize losses and restoration time, and diminish adverse impacts on society. The goal of power system restoration research is to find fast and reliable ways to restore a power system to its normal operational state after a black-out event. The purpose of this paper is to provide a conceptually computational methodology for ensuring the system restoration strategies in a faster manner. To achieve a faster restoration process, new black start generators can be installed allowing network reconfigurations and the load recovery can also be adopted in accelerating the system restoration. In this study to develop more effective and fast restoration in the interconnected power system by

computing various Power System Restoration Indices (PSRI) for two-area interconnected thermal-hydro and thermal-diesel power system in a restructured environment. From the simulated results it is observed that the restoration process for the system with diesel units ensures improved PSRI which provides good margin of stability.

2. TEST SYSTEM FOR AGC IN RESTRUCTURED POWER SYSTEM

AGC in restructured power system having three possible contracts, such as Poolco based transaction, bilateral transactions, and hybrid transaction. In Poolco based transaction contract between Gencos and Discos in same area and in the case of bilateral contract any Discos have the freedom to choose any Gencos in their own area or any other control area. In order to meet the various types of contracts in restructured power system is visualized through disco participation matrix (DPM) [7]. The number of rows and columns in a DPM represents the number of Gencos and Discos respectively [7]. Each entry in the DPM is noted as Contract Participation Factor (CPF), which represents the fraction of total power contracted by j^{th} Disco from i^{th} Genco. Considered first test system, Fig.1 shows the restructured model of a two area hydro-thermal system in which area-1 consists of two thermal Gencos and two Discos and area-2 consists of one themal Gencos and one hydro Gencos and two DISCOs. Fig 2 shows the second test system, the restructured model of a two area thermal diesel system in which area-1 consists of two thermal Gencos and two Discos and area-2 consists of one themal Gencos and one diesel Gencos and two DISCOs. Consider the first system the corresponding DPM will become

$$DPM = \begin{bmatrix} cpf_{11} & cpf_{12} & cpf_{13} & cpf_{14} \\ cpf_{21} & cpf_{22} & cpf_{23} & cpf_{24} \\ cpf_{31} & cpf_{32} & cpf_{33} & cpf_{34} \\ cpf_{41} & cpf_{42} & cpf_{43} & cpf_{44} \end{bmatrix} \quad (1)$$

where *cpf* represents "Contract Participation Factor" and is like signals that carry information as to which the Genco has to follow the load demanded the Disco. The actual and scheduled steady state power flow through the tie-line are given

$$\Delta P_{tie1-2,\,scheduled} = \sum_{i=1}^{2}\sum_{j=3}^{4} cpf_{ij}\,\Delta P_{Lj} - \sum_{i=3}^{4}\sum_{j=1}^{2} cpf_{ij}\,\Delta P_{Lj} \quad (2)$$

$$\Delta P_{tie\,1-2,\,actual} = \left(2\pi T_{12}/s\right)\left(\Delta F_1 - \Delta F_2\right) \quad (3)$$

And at any given time, the tie-line power error $\Delta P_{tie\,1-2,\,error}$ is defined as

$$\Delta P_{tie1-2,\,error} = \Delta P_{tie1-2,\,actual} - \Delta P_{tie1-2,\,scheduled} \quad (4)$$

The error signal is used to generate the respective ACE signals as in the traditional scenario

$$ACE_1 = \beta_1 \Delta F_1 + \Delta P_{tie\,1-2,\,error} \quad (5)$$

$$ACE_2 = \beta_2 \Delta F_2 + \Delta P_{tie\,2-1,\,error} \quad (6)$$

For two area system as shown in Fig.1, the contracted power supplied by i^{th} Genco is

$$\Delta Pg_i = \sum_{j=1}^{DISCO=4} cpf_{ij}\Delta P_{Lj} \quad (7)$$

Also note that $\Delta P_{L1,LOC} = \Delta P_{L1} + \Delta P_{L2}$, $\Delta P_{L2,LOC} = \Delta P_{L3} + \Delta P_{L4}$. In the proposed AGC implementation, the contracted load is fed forward through the DPM matrix to Genco set points. The actual loads affect system dynamics via the input $\Delta P_{L,LOC}$ to the power system blocks. Any mismatch between actual and contracted demands will result in frequency deviations that will drive LFC to re-dispatch the Gencos according to ACE participation factors, i.e., apf_{11}, apf_{12}, apf_{21} and apf_{22}. The proposed PDFF controllers are design using FPA and implemented two-types of test system such as two-area thermal-thermal and thermal-diesel power system and are compared with the output responses of the system considered with the PI controllers. The detailed small perturbation transfer function block diagram model of the two-area thermal- themal and thermal-diesel interconnected power system is shown in Fig.2 and Fig.3.

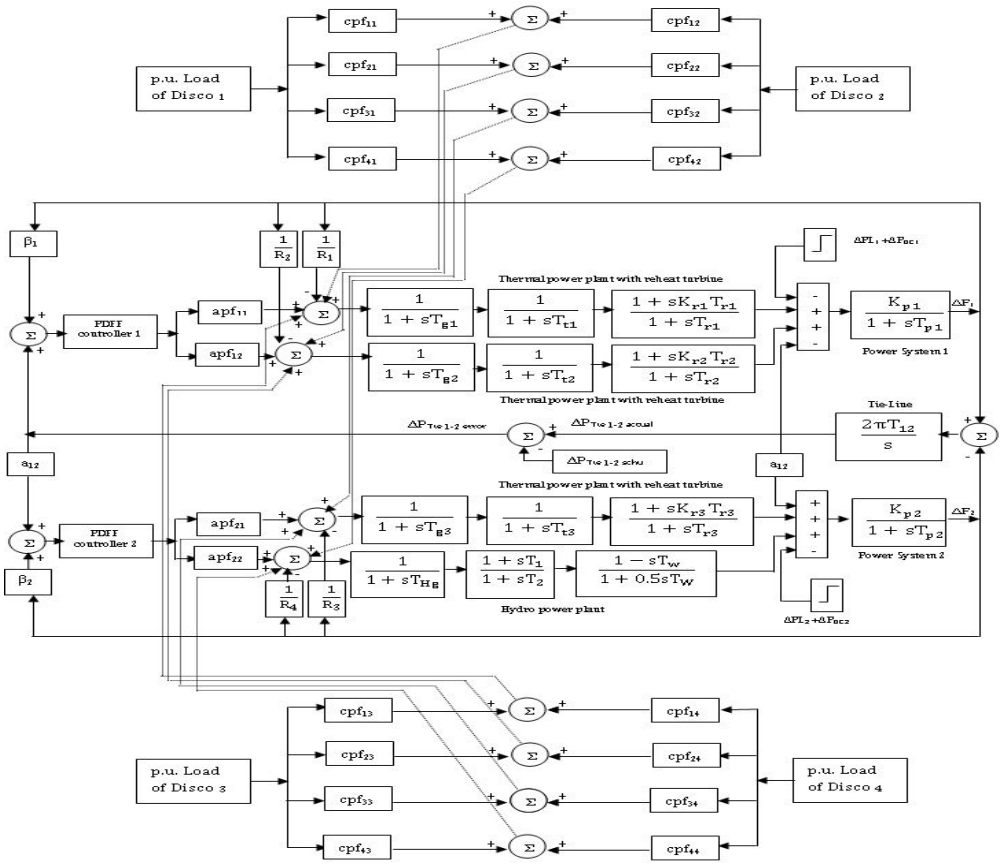

Fig. 1 Linearized model of a two-area hydro-thermal interconnected power system in a restructured environment

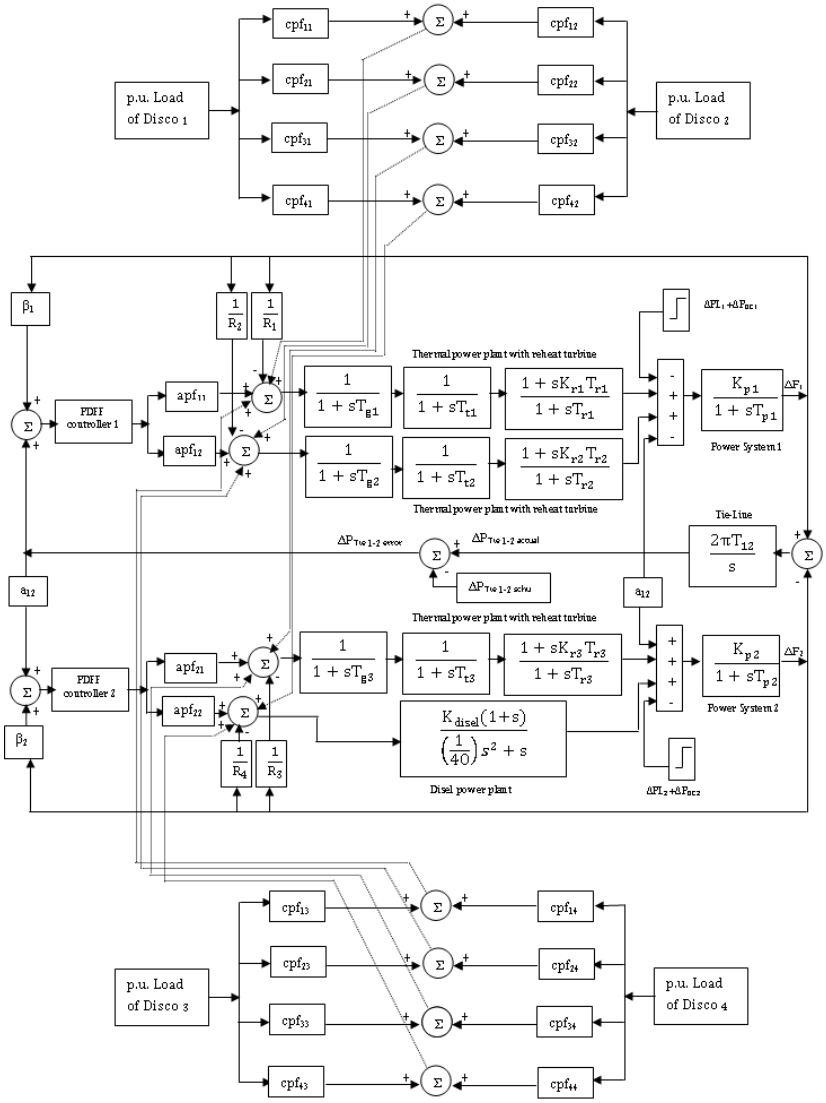

Fig. 2 Linearized model of a two-area thermal-diesel interconnected power system in a restructured environment

3. DESIGN OF PDFF CONTROLLERS USING FPA

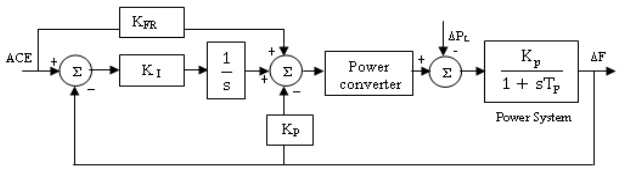

Fig. 3 Block diagram for PDFF control

In PI controller K_P provides stability and high frequency response and K_I ensures that the average error is driven to zero. So no long term error, as the two gains are tuned. This normally provides high responsive systems. But the predominant weakness of PI controller is it often produces excessive overshoot to a step command. The PI controller lacks a windup function to control the integral value during saturation. In this work the use of PDFF-controller which modifies PI, allowing the user to eliminate overshoot and provide much more DC stiffness than PI controller.

Fig. 3 shows a PDFF controller. Like the PI controller, it has an integral gain (K_I) and a proportional gain (K_P). PDFF adds the gain K_{FR}, which allows the user to raise the integral gain in some applications. When an application requires the maximum responsiveness, you don't need much integral gain. Here, you set K_{FR} high. When the application requires maximum low-frequency stiffness, set K_{FR} low; this allows much higher integral gain without inducing overshoot. Unfortunately, it also makes the system slower in responding to the command. The majority of motion control applications are in the middle and K_{FR} = 65% usually gives good results. In this study K_{FR} set to 0.65 then K_P and K_I value are tuned using Flower Pollination Algorithm (FPA) technique. The main function of AGC is to control load frequency and tie line power during load disturbance. So the error signals of frequency and tie line power are used as design criteria to tune the PI controller. An objective function is created which uses the variables of the population from FPA, passes through a model containing two area power system and obtains the error signals frequency and tie line power. The performance of these responses is measured using performance functions such as Integral of Squared Error (ISE) given by Eqs (8)

$$J = \int_0^{t_{sim}} (\Delta F_1^2 + \Delta F_2^2 + \Delta P_{tie}^2)\, dt \qquad (8)$$

3.1 Flower Pollination Algorithm

Yang [14] emulated the characteristic of the biological flower pollination in flowering plant to develop single objective FPA based on the rules listed as follows:

(i) The global pollination processes are biotic and cross pollination through which the pollen transports pollinators perform the levy flight, (ii) Local pollination is viewed as abiotic and self pollination. (iii) Reproduction probability is considered as flower constancy which is proportional to the resemblance of the two flowers in concerned and (iv) The switching probability controlled both the local and global pollination $p \in [0, 1]$. Local pollination can have fraction p that is significant in the entire processes of the pollination because of physical proximity and wind. The plant can possess multiple flowers and every flower patch typically emits millions or even billions of pollen gametes in real life pollination practice. To simplify the proposed algorithm development, it was assumed that each plant has a single flower and each flower emit only a single pollen gamete. This result to the elimination of the need to differentiate pollen gamete, plant or solution to a problem. This means that a solution *xi* to a problem is equivalent to a flower and pollen gamete. The major stages in the design of SFPA are global and local pollination. In the global pollination, the pollens of the flowers are moved by pollinators e.g. insects and pollens can move for a long distance since the insects typically fly for a long range of distances. This process guarantees pollination and reproduction of the fittest solution represented as g*. The flower constancy can be represented as:

$$x_i^{t+1} = x_i^t + L(x_i^t - g_*) \qquad (9)$$

where x_i^t is the pollen i or solution vector x_i at iteration t, and g_* is the current best solution found among all solutions at the current generation/iteration. The parameter L is the strength of the pollination, which essentially is a step size. Since insects may move over a long distance with various distance steps, which is mimicked by levy distribution of flight [14, 15] and mathematically represented as

$$L \sim \frac{\lambda \Gamma(\lambda) \sin\left(\frac{\pi\lambda}{2}\right)}{\pi} \frac{1}{s^{1+\lambda}} \qquad (s \ll s_0 > 0) \qquad (10)$$

where $\Gamma(\lambda)$ is the standard gamma function, and this distribution is valid for large steps s > 0. The local pollination and flower constancy can be represented as

$$x_i^{t+1} = x_i^t + \varepsilon(x_j^t - x_k^t) \qquad (11)$$

where x_j^t and x_k^t represent pollen from different flowers of the same species of plant. Thus, mimic the flower constancy in a limited neighborhood. The switch probability or proximity probability is used to switch between common global pollination to intensive local pollination. The effectiveness of the FPA can be attributed to the following two reasons: (i) Insect pollinators can travel in long distances which enable the FPA to avoid local landscape to search in a very large space (explorations). (ii) The FPA ensures that similar species of the flowers are consistently chosen which guarantee fast

convergence to the optimal solution (exploitation). The proposed flower pollination algorithm for solving AGC application

(i) Step 1: Initialize the objective function as given in the equation (8)

(ii) Step 2: Initialize a population of x = (x_1, x_2 ...x_{NF}) flowers/pollen gametes with the population size of *NF x N*. Where *NF* is the number of flowers as 30 and *N* is the dimension size depends on the number of controller gain values for each area in the two area system. In this study *N* is equal to four because PI controller is used to in each area (K_{P1}, K_{I1} K_{P2}, K_{I2}) and calculate the Fitness for each solutions.

(iii) Step 3: Find the best solution to the initial population and define a switch probability p ∈ [0, 1] and define a stopping criterion (a fixed number of generations/iterations)

(iv) Step 4: while (t <Maximum Generation) for i = 1 : n (all n flowers in the population) if rand < p, Draw a (d-dimensional) step vector *L* which obeys a Levy distribution Global pollination has been done using equation (9). Else draw from a uniform distribution in [0, 1].

Randomly choose j^{th} and k^{th} flower among all the solutions and do local pollination through equation (11), end if

(v) Step 5: Evaluate new solutions using the objective function. If new solutions are better, update them in the population, end for

(vi) Step 6: Find the current best solution based on the objective fitness value, end while.

4. POWER SYSTEM RESTORATION

The system restoration strategies are found closely related to the systems' characteristics. After analyzing the system conditions and characteristics of outages, system restoration planners or dispatchers will select the Power System Restoration Indices (PSRI) which were obtained based on system dynamic performances and the remedial measures to be taken can be adjudged. In this study two-area thermal-thermal and thermal-diesel interconnected power system in a restructured environment are considered when the system is operating in a normal condition with Gencos units in operation and are one or more Gencos unit outage in any area. From these Restoration Indices the restorative measures like the magnitude of control input, rate of change of control input required can be adjudged. The various power system restoration indices $(PSRI_1, PSRI_2, PSRI_3 \text{ and } PSRI_4)$ are calculated as follows

Step 1: The Power System Restoration Index 1 $(PSRI_1)$ is obtained from the ratio between the settling time of the control input deviation $\Delta P_{c1}(\tau_{s1})$ response of area 1 and power system time constant (T_{p1}) of area 1

$$PSRI_1 = \frac{\Delta P_{c1}(\tau_{s1})}{T_{p1}} \quad (12)$$

Step 2: The Power System Restoration Index 2 $(PSRI_2)$ is obtained from the ratio between the settling time of the control input deviation $\Delta P_{c2}(\tau_{s2})$ response of area 2 and power system time constant (T_{p2}) of area 2

$$PSRI_2 = \frac{\Delta P_{c2}(\tau_{s2})}{T_{p2}} \quad (13)$$

Step 3: The Power System Restoration Index 3 $(PSRI_3)$ is obtained from the peak value of the control input deviation $\Delta P_{c1}(\tau_p)$ response of area 1 with respect to the final value $\Delta P_{c1}(\tau_s)$

$$PSRI_3 = \Delta P_{c1}(\tau_p) - \Delta P_{c1}(\tau_s) \quad (14)$$

Step 4: The Power System Restoration Index 4 $(PSRI_4)$ is obtained from the peak value of the control input deviation $\Delta P_{c2}(\tau_p)$ response of area 1 with respect to the final value $\Delta P_{c1}(\tau_s)$

$$PSRI_4 = \Delta P_{c2}(\tau_p) - \Delta P_{c2}(\tau_s) \quad (15)$$

5. SIMULATION RESULTS AND OBSERVATIONS

In this study two types of test system such as two-area interconnected Hydro-thermal and thermal-diesel power system is considered. Both system have two generating unit in each area with same capacities is considered. The model of the system under study has been developed in MATLAB/SIMULINK environment. The nominal parameters are given in Appendix. In this work, Flower Pollination Algorithm (FPA) is used to tune the PDFF controller for a two- area interconnected

power system. Proportional gain constant (K_P), Integral gain constant (K_I), are considered as variables describing a population defined in an FPA and K_{FR}=0.65. The optimal solution of control inputs is taken an optimization problem and the cost function in Eq(8) is derived using the frequency deviations of control areas and tie-line power changes which uses the design criteria to calculate the flower constancy of the defined population. The parameter *p* defines the amount of local search and global search for FPA. To choose this parameter, the proposed method is simulated for various values and that simulated for *p* varies from 0.1 to 1 with step change of *p* with step size 0:01 in the range of 0.1 to 1. The optimum PDFF controller gain values for two type of test systems are tuned for various case studies are listed in the Table1 and 2. These PDFF controllers are implemented in a proposed power system for different types of transactions and compared with PI controller. The dynamic ouput response of the hydro-thermal system is shown in Fig 4 and results are tabulated in Table3. From Fig 4 and Tables 3, it can be observed that the proposed PDFF controller show better performance as compared with PI controller.

Scenario 1: Poolco based transaction

In this scenario, Gencos participate only in the load following control of their areas. It is assumed that a large step load 0.1 pu MW is demanded by each Disco in area 1. Assume that a case of Poolco based contracts between Dicos and available Gencos is simulated based on the following Disco Participation Matrix (DPM) referring to Eq (1) is considered as

$$DPM = \begin{bmatrix} 0.5 & 0.5 & 0.0 & 0.0 \\ 0.5 & 0.5 & 0.0 & 0.0 \\ 0.0 & 0.0 & 0.0 & 0.0 \\ 0.0 & 0.0 & 0.0 & 0.0 \end{bmatrix} \quad (16)$$

$Disco_1$ and $Disco_2$ demand identically from their local Gencos, viz., $Genco_1$ and $Genco_2$. Therefore, cpf_{11} = cpf_{12} = 0.5 and cpf_{21} = cpf_{22} = 0.5. It may happen that a Disco violates a contract by demanding more power than that specified in the contract and this excess power is not contracted to any of the Gencos. This uncontracted power must be supplied by the Gencos in the same area to the Disco. It is represented as a local load of the area but not as the contract demand. Consider scenario-1 again with a modification that Disco demands as given in Table 1 and 2. From the simulation results Power System Restoration Indices are evaluated using Eq (12)-(15) from dynamic responses of the control input deviations of the proposed test system is shown in Table 4 (case 1- 4).

Scenario 2: Bilateral transaction

Here all the Discos have contract with the Gencos and the following Disco Participation Matrix (DPM) referring to Eq (1) is considered as

$$DPM = \begin{bmatrix} 0.4 & 0.2 & 0.4 & 0.5 \\ 0.1 & 0.3 & 0.2 & 0.3 \\ 0.3 & 0.2 & 0.2 & 0.1 \\ 0.2 & 0.3 & 0.2 & 0.2 \end{bmatrix} \quad (17)$$

In this case, the $Disco_1$, $Disco_2$, $Disco_3$ and $Disco_4$, demands 0.15 pu.MW, 0.05 pu.MW, 0.15 pu.MW and 0.05 pu.MW from Gencos as defined by cpf in the DPM matrix and each Gencos participates in AGC as defined by the following ACE participation factor apf_{11} = apf_{12} = 0.5 and apf_{21} = apf_{22} = 0.5. The corresponding PSRI are calculated using Eq (12)-(15) from dynamic responses of control input deviations of the proposed test system are shown in Table 4 (case 5- 8). Apart from the normal operating condition of the test systems few other case studies like outage generating unit in any area and uncontracted power demand in any area during outage is considered. In this study $Genco_2$ in area 1 is outage and uncontracted power demand in any area and Disco Participation Matrix Eq (17) is considered. The optimum PDFF controller gain values for two test system are tuned for various case studies are tabulated in the Table 1and 2 (case 9-12). These PDFF controllers are implemented in a proposed two types test system for different type of transactions. From simulation results the dynamic responses of control input deviations of the proposed test system the corresponding PSRI using Eq (12)-(15) and tabulated in Table 4 (case 9- 12). From these Restoration Indices the restorative measures like the magnitude of control input, rate of change of control input required can be adjudged. From the simulated results is shown in Fig 5, it is observed

that the restoration process with the diesel unit ensures not only reliable operation but provides a good margin of stability compared with that of a Hydro Turbine with Mechanical Governor.

5.1. Power System Restoration Assessment

The main focus in this paper PSRI are useful for system planners for restoration planning in advance.

(i) If $1.0 \leq PSRI_1, PSR$, then the system subject to a large steady error for step load changes. The integral control action is required based on the performance criteria. The integral controller gain of each control area has to be increased causing the speed changer valve to open up widely. Thus the speed- changer position attains a constant value only when the frequency error is reduced to zero.

(ii) If $PSRI_1, PSR$, then the system required more amount of distributed generation requirement is needed and the FACTS devices are needed to improvement tie-line power oscillations.

(iii) If $0.05 \leq PSRI_3, PSR$, then the system required the stabilization of frequency oscillations in an interconnected power system. The conventional load-frequency controller may no longer be able to attenuate the large frequency oscillation due to the slow response of the governor for unpredictable load variations. Thus continuing change in power system configurations and their operating conditions might lead to undesired operation of relays. So that in deregulated system, regulation and load following are the two frequency-related ancillary services required for balancing the varying load with matching generation. In cases where a dramatic decline in frequency occurs during the restoration process, it is necessary to reduce the amount of load that are connected, which can be accomplished by the application of under load shedding scheme.

(iv) If $PSRI_3, PSR$, then the system is vulnerable and the system becomes unstable and may result to blackout. To restore the system as quickly as possible, especially for a bulk system, partitioning system into islands is necessary. Islands are resynchronizes after restoration of each island. Major actions involved in this restoration process are start up of black start units, cranking of non-black start units, restoration of islands, and synchronization of islands.

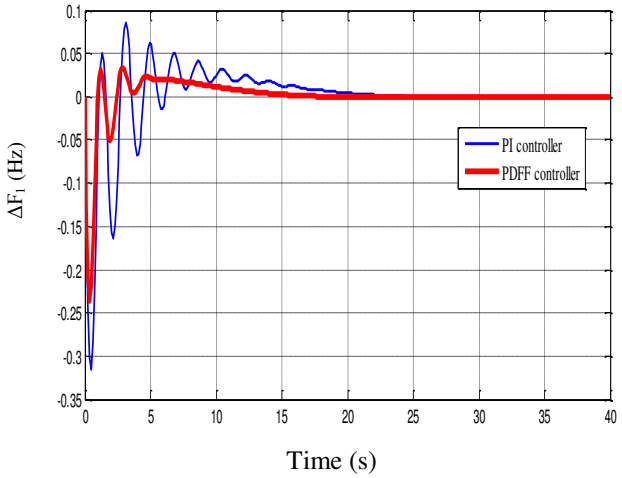

Fig. 4(a) ΔF_1 (Hz) Vs Time(s)

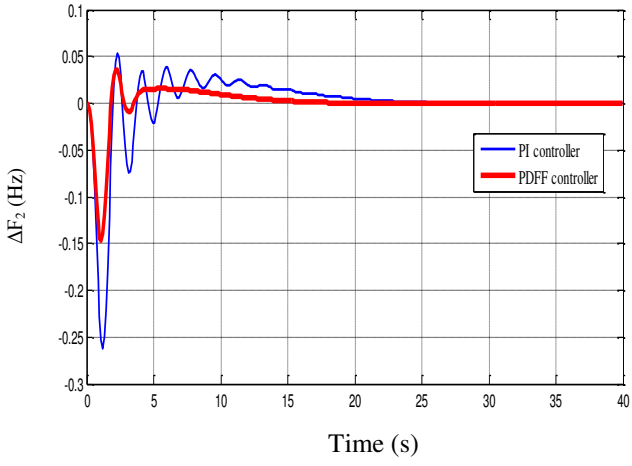

Fig. 4(c) $\Delta Ptie_{12,\ actual}$ (p.u.MW) Vs Time (s)

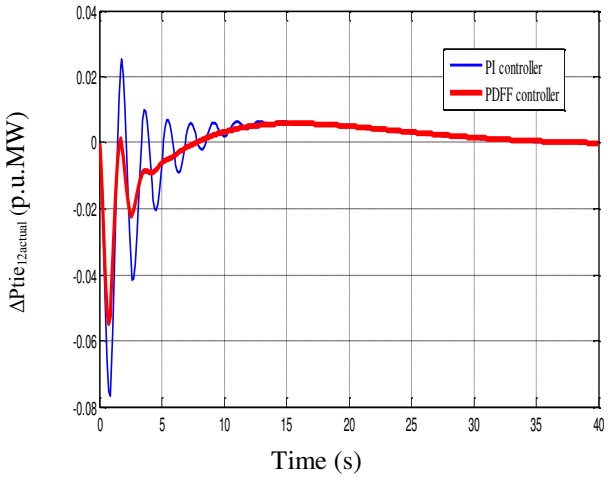

Fig. 4(c) $\Delta Ptie_{12,\ actual}$ (p.u.MW) Vs Time (s)

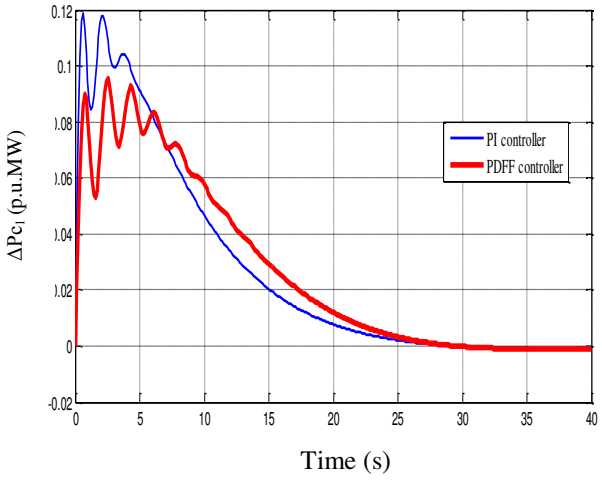

Fig. 4(d) ΔPc_1 (p.u.MW) Vs Time (s)

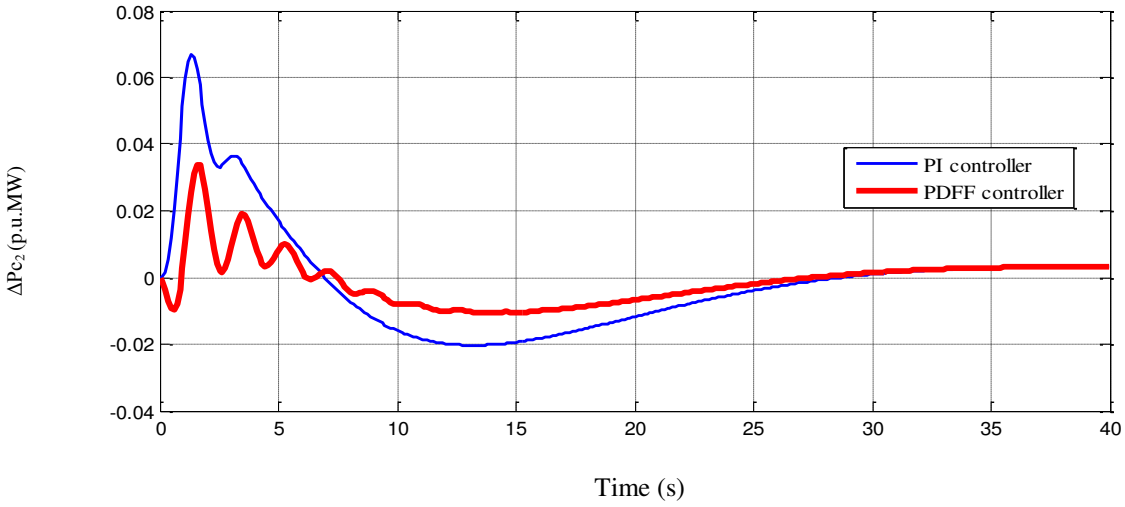

Fig. 4(e) ΔPc_2 (p.u.MW) Vs Time (s)

Fig.4 Dynamic responses of the frequency deviations, tie- line power deviations, and Control input deviations for a two area hydro-thermal system using PI and PDFF controllers (case-1)

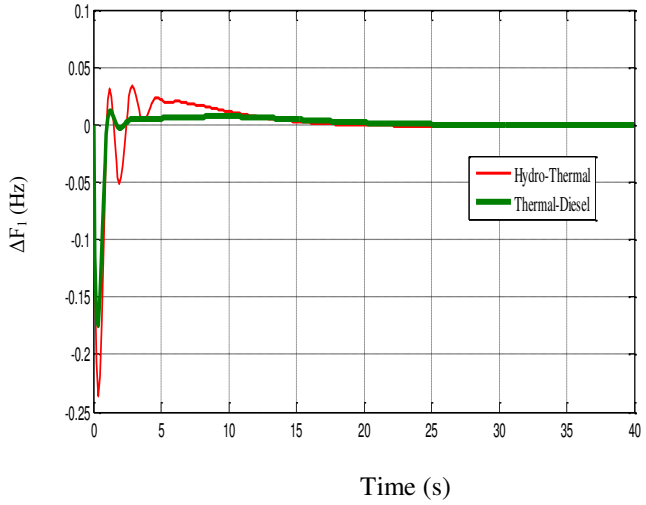

Fig. 5(a) ΔF_1 (Hz) Vs Time(s)

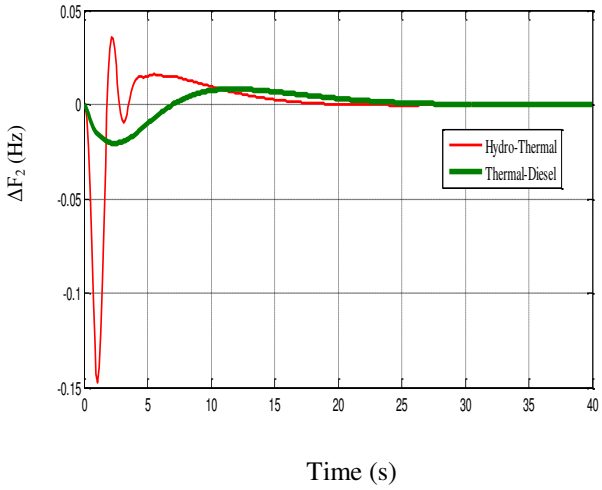

Fig. 5(b) ΔF_2 (Hz) Vs Time (s)

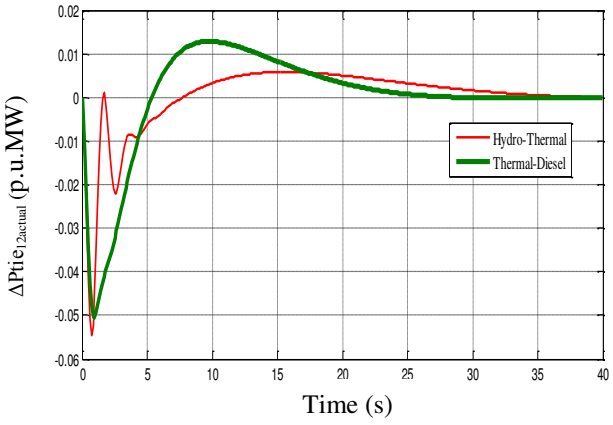

Fig. 5(c) $\Delta Ptie_{12,\ actual}$ (p.u.MW) Vs Time (s)

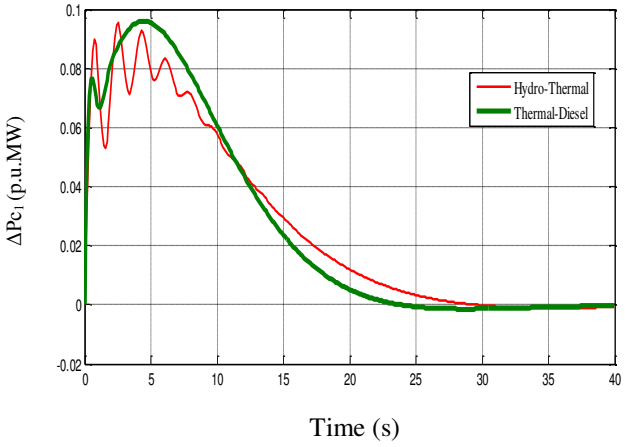

Fig. 5(d) ΔPc_1 (p.u.MW) Vs Time (s)

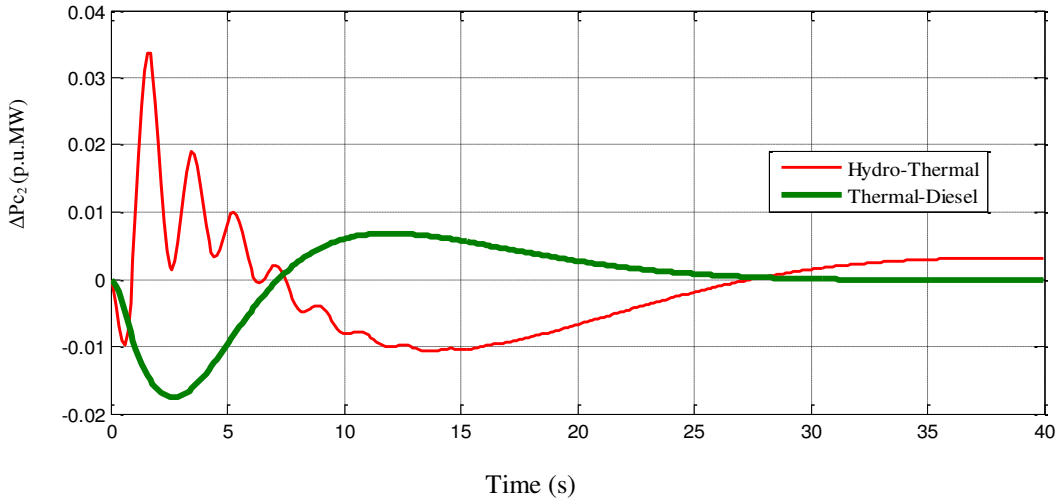

Fig. 5(e) ΔPc_2 (p.u.MW) Vs Time (s)

Fig.5 Dynamic responses of the frequency deviations, tie- line power deviations, and Control input deviations for a two area thermal-Diesel system using PDFF controllers (case-1)

Table 1:

Optimal PDFF controller gain values using FPA for two-area reheat hydro- thermal power system with corresponding Load demand change

Two-area hydro-thermal system	PDFF controller gain of area 1		PDFF controller gain of area 2		Load demand in pu.MW				un contracted load demand pu.MW	
	K_P	K_I	K_P	K_I	$Disco_1$	$Disco_2$	$Disco_3$	$Disco_4$	area1	area 2
Case 1	0.294	0.405	0.252	0.343	0.1	0.1	0.0	0.0	0.0	0.0
Case 2	0.312	0.435	0.261	0.348	0.1	0.1	0.0	0.0	0.05	0.0
Case 3	0.343	0.421	0.276	0.327	0.1	0.1	0.0	0.0	0.0	0.05
Case 4	0.367	0.481	0.281	0.354	0.1	0.1	0.0	0.0	0.05	0.05
Case 5	0.304	0.357	0.267	0.351	0.15	0.05	0.15	0.05	0.0	0.0
Case 6	0.311	0.361	0.379	0.353	0.15	0.05	0.15	0.05	0.05	0.0
Case 7	0.326	0.355	0.371	0.363	0.15	0.05	0.15	0.05	0.0	0.05
Case 8	0.397	0.375	0.393	0.375	0.15	0.05	0.15	0.05	0.05	0.05
Case 9	0.324	0.358	0.385	0.378	0.12	0.08	0.12	0.08	0.0	0.0
Case 10	0.346	0.369	0.394	0.425	0.12	0.08	0.12	0.08	0.05	0.0
Case 11	0.351	0.396	0.395	0.469	0.12	0.08	0.12	0.08	0.0	0.05
Case 12	0.367	0.427	0.401	0.471	0.12	0.08	0.12	0.08	0.05	0.05

Table 2:

Optimal PDFF controller gain values using FPA for two-area reheat thermal-diesel power system with corresponding Load demand change

Two-area thermal-diesel system	PDFF controller gain of area 1		PDFF controller gain of area 2		Load demand in pu.MW				Uncontracted load demand pu.MW	
	K_P	K_I	K_P	K_I	$Disco_1$	$Disco_2$	$Disco_3$	$Disco_4$	area1	area 2
Case 1	0.242	0.356	0.236	0.313	0.1	0.1	0.0	0.0	0.0	0.0
Case 2	0.273	0.382	0.243	0.317	0.1	0.1	0.0	0.0	0.05	0.0
Case 3	0.301	0.386	0.257	0.302	0.1	0.1	0.0	0.0	0.0	0.05
Case 4	0.312	0.437	0.265	0.327	0.1	0.1	0.0	0.0	0.05	0.05
Case 5	0.267	0.306	0.243	0.339	0.15	0.05	0.15	0.05	0.0	0.0
Case 6	0.269	0.322	0.357	0.337	0.15	0.05	0.15	0.05	0.05	0.0
Case 7	0.272	0.309	0.353	0.345	0.15	0.05	0.15	0.05	0.0	0.05
Case 8	0.345	0.327	0.373	0.357	0.15	0.05	0.15	0.05	0.05	0.05
Case 9	0.287	0.306	0.362	0.353	0.12	0.08	0.12	0.08	0.0	0.0
Case 10	0.292	0.317	0.373	0.401	0.12	0.08	0.12	0.08	0.05	0.0
Case 11	0.306	0.346	0.378	0.443	0.12	0.08	0.12	0.08	0.0	0.05
Case 12	0.383	0.262	0.379	0.384	0.12	0.08	0.12	0.08	0.05	0.05

Table 3:

Comparison of the dynamic performance for test system (case-1)

Test system	Setting time (τ_s) in sec			Peak over / under shoot		
	ΔF_1	ΔF_2	ΔP_{tie}	ΔF_1 in Hz	ΔF_2 in Hz	ΔP_{tie} in p.u.MW
Hydro-Thermal system Using PI controller	25.9	22.8	38.4	0.315	0.261	0.077
Hydro-Thermal system Using PDFF controller	20.5	18.6	35.7	0.239	0.147	0.054
Thermal-diesel system Using PDFF controller	18.5	15.7	30.4	0.139	0.022	0.049

Table 4:

PSRI for two-area interconnected power system using FPA based PDFF controller

Load demand change	PSRI for Hydro-thermal power system considering apf_{11} =apf_{12} = apf_{21} = apf_{22}= 0.5					PSRI for thermal-diesel power system considering apf_{11} =apf_{12} = apf_{21} =$apf_{22=}$ 0.5				
	$PSRI_1$	$PSRI_2$	$PSRI_3$	$PSRI_4$	$\int PC_2$	$PSRI_1$	$PSRI_2$	$PSRI_3$	$PSRI_4$	$\int PC_2$
Case 1	1.595	1.508	0.095	0.031	0.264	1.452	1.401	0.084	0.017	0.132
Case 2	1.845	1.623	0.108	0.032	0.345	1.737	1.517	0.104	0.018	0.223
Case 3	1.784	1.678	0.096	0.036	3.467	1.673	1.572	0.093	0.021	3.333
Case 4	2.237	2.073	0.127	0.043	3.872	2.117	2.013	0.124	0.028	3.718
Case 5	1.478	1.578	0.091	0.032	1.784	1.352	1.461	0.088	0.012	1.637
Case 6	1.547	1.789	0.109	0.037	1.687	1.431	1.672	0.107	0.022	1.528
Case 7	1.758	1.875	0.104	0.039	3.523	1.647	1.771	0.103	0.024	3.389
Case 8	1.845	1.978	0.112	0.041	3.124	1.733	1.873	0.109	0.035	3.012
Case 9	2.051	2.278	1.142	0.057	1.437	1.964	2.171	1.138	0.042	1.314
Case 10	2.127	2.378	1.157	0.058	1.594	2.017	2.264	1.155	0.043	1.488
Case 11	2.347	2.458	1.158	0.059	3.696	2.231	2.354	1.156	0.044	3.572
Case 12	2.972	2.879	1.245	0.061	3.688	2.754	2.762	1.239	0.053	3.573

6. Conclusion

The PDFF controllers are designed using FPA technique and implemented in two area interconnected power system for different types transactions. The effectiveness of the proposed method is tested in a two-area hydro-thermal and thermal-diesel deregulated power system for a wide range of load demands and disturbances under different operating conditions. The results have demonstrated the superiority of the FPA for finding the global optimum solution. The results also indicate that FPA is more accurate, reliable and efficient in finding global optimal solution than other algorithms. The proposed PDFF controller shows better performance to ensure improved PSRI in order to provide reduce the restoration time, thereby improving the system reliability than PI controller. The traditional role of the diesel power plant as fast response unit, ideal for improving primary control response of the power system has been to a certain extent lost, due to relatively high constraints in ramping up and down the power output during the normal operation.

ACKNOWLEDGEMENT

The authors wish to thank the authorities of Annamalai University, Annamalainagar, Tamilnadu, India for the facilities provided to prepare this paper.

REFERENCES

[1] Abhijith pappachen and Peer Fathima, Critical research areas on load frequency control issues in a deregulated power system: A state-of-the-art-of-review, Renewable and Sustainable Energy Reviews, 72 (2017), 163-177.

[2] Shital M. Pujara and Chetan D. Kotwal, An Inclusive Review on Load Frequency Control in Deregulated Market, International Journal on Electrical Engineering and Informatics, 8(3) (2016) 595-611.

[3] Anu Chaudhary, Mohan Kashyap, Satish Kansal, Automatic Generation Control - A Review, IJSRSET ISSN : 2394-4099, 2 (2) (2016) 81-84.

[4] Ibraheem, Omveer Singh, Current Philosophies of Intelligent Techniques based AGC for Interconnected Power Systems, International Journal of Energy Engineering (IJEE), 4 (3) (2014) 141-150

[5] Tyagi B, Srivastava SC. A decentralized automatic generation control scheme for competitive electricity markets. IEEE Trans Power Syst 2006;21(1):312–20.

[6] Sekhar GTC, Sahu RK, Baliarsingh AK, Panda S. Load frequency control of power system under deregulated environment using optimal firefly algorithm. Int JElectr Power Energy Syst 2016;74:195–211.

[7] V. Donde, M. A. Pai, I. A. Hiskens, Simulation and optimization in an AGC system after deregulation, IEEE Transactions on Power Systems 16 (3) (2001) 481-489.

[8] H. Shayeghi, A. Jalili, H.A. Shayanfar, Multi-stage fuzzy load frequency control using PSO, Energy Convers. Manage. 49 (2008) 2570–2580.

[9] A. Demiroren and H. L. Zeynelgil, GA Application to Optimization of AGC in Three-area Power System after Deregulation, International Journal of Electrical Power & Energy Systems, 29 (2007) 230-240

[10] D. Guha, P.K. Roy, S. Banerjee, Optimal design of superconducting magnetic energy storage based multi-area hydro-thermal system using biogeography based optimization, in: Proc. 2014 IEEE Fourth Int. Conf. Emerging Application of Information Technology (EAIT-2014), ISI Kolkata, 2014, pp. 52–57.

[11] A. H. Gandomi and A. H. Alavi, Krill herd: a new bio-inspired optimization algorithm, Communications in Nonlinear Science and Numerical Simulation, 7(12) (2012) 4831-4845.

[12] R.K. Sahu, T.S. Gorripotu, S. Panda, Automatic Generation Control Of Multi-Area Power Systems With Diverse Energy Sources using Teaching Learning Based

Optimization Algorithm, Eng. Sci. Technol. Int. J. 19 (2016) 113–134.

[13] B.Paramasivam and I.A.Chidambaram, Bacterial Foraging Optimization Based Load Frequency Control of Interconnected Power Systems with Static Synchronous Series Compensator, International Journal of Latest Trends in Computing, 1(2) (2010) 7-13.

[14] Yang X-S. Flower pollination algorithm for global optimization. Berlin Heidelberg: Springer; 2012.

[15] Yang X-S, Karamanoglu M, He X., Flower pollination algorithm: a novel approach for multi objective optimization, Engineering Optimization, 46(9) (2014) 1222–1237.

[16] Satya Dinesh Madasu, M.L.S. Sai Kumar, Arun Kumar Singh, A flower pollination algorithm based automatic generation control of interconnected power system, Ain Shams Engineering Journal (2016), DOI:10.1016/j.asej.2016.06.003, accepted for publications on 8th June 2016

[17] Lalit Chandra Saikia, J.Nanda, S.Mishra, Performance comparison of several classical controllers in AGC for multi-area interconnected thermal system, International Journal of Electrical Power & Energy Systems, 33 (2011) 394-401.

[18] Yutian Liu, Rui Fan, Vladimir Terzija, Power system restoration: a literature review from 2006 to 2016, J. Mod. Power Syst. Clean Energy, (2016) 4(3): 332–341.

[19] A. Jalili, H. Shayeghi, N.M. Tabatabaei, Fuzzy PID controller base on LFC in the deregulated power system including SMES, International Journal on Technical and Physical Problems of Engineering, Vol.3, No.3, pp.38-47, 2011.

APPENDIX – A

Data for the interconnected two- area interconnected Power System [19]

Rating of each area = 2000 MW, Base power = 2000 MVA, f^o = 60 Hz, $R_1 = R_2 = R_3 = R_4$ = 2.4 Hz / p.u.MW, $T_{g1} = T_{g2} = T_{g3} = T_{g4}$ = 0.08 s, $T_{r1} = T_{r2} = T_{r1} = T_{r2}$ = 10 s, $T_{t1} = T_{t2} = T_{t3} = T_{t4}$ = 0.3 s, $K_{p1} = K_{p2}$ = 120Hz/p.u.MW, $T_{p1} = T_{p2}$ = 20 s, $\beta_1 = \beta_2$ = 0.425 p.u.MW / Hz, $K_{r1} = K_{r2} = K_{r3} = K_{r4}$ = 0.5, T_{Hg} =0.2s, T_1=0.513s, T_2=10s, T_w=1s, K_{diesel} =16.5, $2\pi T_{12}$ = 0.545 p.u.MW / Hz, a_{12} = -1